A proton pump enhancing photosynthesis links phagocytosis to marine phytoplankton symbiogenesis

Daniel P. Yee[1*], Ty J. Samo[2], Raffaela M. Abbriano[1], Bethany Shimasaki[1], Maria Vernet[1], Xavier Mayali[2], Peter K. Weber[2], B. Greg Mitchell[1], Mark Hildebrand[1], Martin Tresguerres[1*]

Affiliations:

[1]Scripps Institution of Oceanography, University of California San Diego; 9500 Gilman Drive, La Jolla, California

[2]Lawrence Livermore National Laboratory, Physical and Life Sciences Directorate; 7000 East Avenue, Livermore, California

*Corresponding authors. Email: daniel.p.yee@gmail.com, mtresguerres@ucsd.edu

Abstract: The chloroplasts of most marine eukaryotic phytoplankton are surrounded by intracellular membranes derived from ancestral secondary endosymbiotic events between heterotrophic unicellular eukaryotes and red microalgae. We report that the proton-pumping enzyme V-type H^+-ATPase (VHA), ubiquitously used in eukaryotic intercellular digestion, is localized around chloroplasts of centric diatoms where VHA-activity significantly enhances photosynthesis over the full range of oceanic irradiances. Similar results in pennate diatoms, dinoflagellates, and coccolithophorids, but not green or red microalgae, imply a shared VHA-dependent mechanism in secondary endosymbiotic phytoplankton that enhances photosynthesis and conservatively contributes 7% of primary production in the ocean. Analogous VHA-dependent mechanisms in extant photosymbiotic marine invertebrates provide evidence for an adaptive advantage throughout the transition from endosymbiosis to symbiogenesis.

One-Sentence Summary: Stimulation of photosynthesis by a conserved proton pump provides a functional link between food digestion and symbiogenesis

Main Text: Diatoms, dinoflagellates, and coccolithophorids are the dominant groups of marine eukaryotic phytoplankton collectively responsible for the majority of the primary production in the ocean (*1*). These phytoplankton originated from secondary endosymbiotic events that started with the phagocytosis of a red alga by a heterotrophic protozoan and, over evolutionary time, culminated in their fusion into single organisms carrying ancestral red chloroplasts (*2*). This symbiogenesis hypothesis is supported by a wealth of palaeontologic, morphologic, and genomic evidence (*3–6*); however, the underlying cellular mechanisms and their functional advantages both to extant phytoplankton and during the transition from endosymbiosis to symbiogenesis remain to be elucidated (*1*, *7*).

Secondary endosymbiotic phytoplankton possess additional intracellular membranes surrounding their chloroplasts, which are hypothesized to derive from the ancestral phagosome that engulfed the red alga (*8*). Since intracellular digestive vacuoles are ubiquitously acidified by V-type H^+-ATPase (VHA) proton pumps (*9*), acidification of the microenvironment around secondary chloroplasts was proposed to promote the dehydration of dissolved inorganic carbon (DIC) into CO_2 thus enhancing photosynthesis (*10*, *11*). Evidence for VHA-enhancement of photosynthesis in phytoplankton has yet to be reported; however, an analogous mechanism has been recently identified in cnidarian and mollusks that establish tertiary phago-photosymbiotic relationships with microalgae (*12–14*). Here, we investigated whether VHA activity enhances photosynthetic O_2 production by extant marine diatoms, dinoflagellates and coccolithophorids, and conducted additional experiments on the diatom *Thalassiosira pseudonana* to confirm the presence of VHA surrounding their chloroplasts and to quantify the contribution of VHA activity to photosynthetic carbon fixation over the full range of environmentally relevant irradiances.

Similar to photosymbiotic cnidarians and mollusks (*12–14*), inhibition of VHA activity induced significant decreases in gross maximum O_2 production in the centric diatom *T. pseudonana*, the pennate diatom *Phaeodactylum tricornutum*, the dinoflagellate *Brandtodinium natricula*, and the coccolithophorid *Emiliania huxleyi*. In contrast, photosynthetic O_2 production by the green alga *Chlorella sp.* or by the red alga *Porphyrydium purpurneum* were not affected by VHA inhibition (Fig. 1; table S1). While these latter two species possess VHA that contribute to vacuole homeostasis (*15–18*), they did not originate by secondary endosymbiosis and therefore lack the intracellular membranes of phagocytic origin that surround the chloroplasts of secondary endosymbiotic phytoplankton.

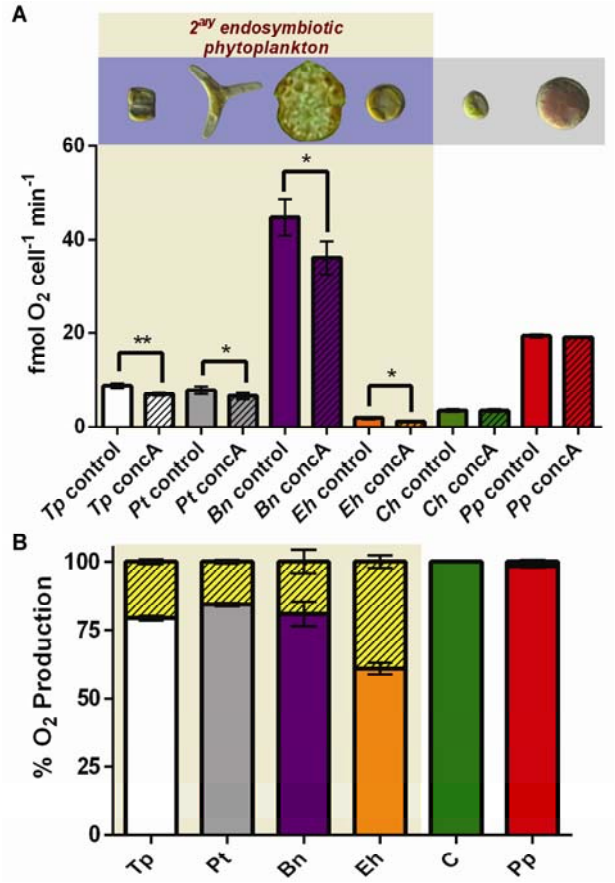

Fig. 1. Contribution of VHA to O_2 production of marine microalgae. (**A**) Gross maximum O_2 production per cell in control (vehicle DMSO; open bars) and VHA-inhibited (concA=10 nM concanamycin A; hatched bars) cultures. (**B**) Percentage of O_2 production that is dependent on VHA activity (yellow hatched area). Tp= *T. pseudonana* (centric diatom); Pt= *P. tricornutum* (pennate diatom); Bn= *Brandtodinium natricula* (dinoflagellate); Eh= *E. huxleyi* (coccolitophorid); C= *Chlorella* sp. (green microalgae); Pp= *P. purpurneum* (red microalgae). Error bars = SEM; n = 3 except *Br* (n=6); Paired *t* test: $*p<0.05$; $**p<0.01$.

We further explored VHA-enhancement of photosynthesis in the model diatom *T. pseudonana*. Transcriptomics analysis on cell-cycle synchronized cultures revealed constitutive expression of all VHA subunits (Fig. 2A-B). However, VHA can have multiple subcellular localizations and participate in diverse processes in addition to intracellular digestion (*19*, *20*). Indeed, we recently showed that VHA localizes to the silica deposition vesicle of *T. pseudonana* during the G2+M phase of cellular division, and that VHA activity is essential for biomineralization of the silica cell wall (*21*). Here, confocal fluorescence super-resolution microscopy of transgenic *T. pseudonana* expressing eGFP-tagged VHA subunit B demonstrated that this proton pump is present around chloroplasts throughout the cell cycle (Fig. 2C & fig. S1). Simultaneous accumulation of the acidotropic fluorescent dye PDMPO (*22*) around chloroplasts implied acidification of the microenvironment to ≤ pH 5.5. At this pH, the majority of DIC exists as CO_2, supporting the quarter-century-old hypothesis that intracellular secondary endosymbiotic membranes play a role in enhancing photosynthesis (*10*, *11*).

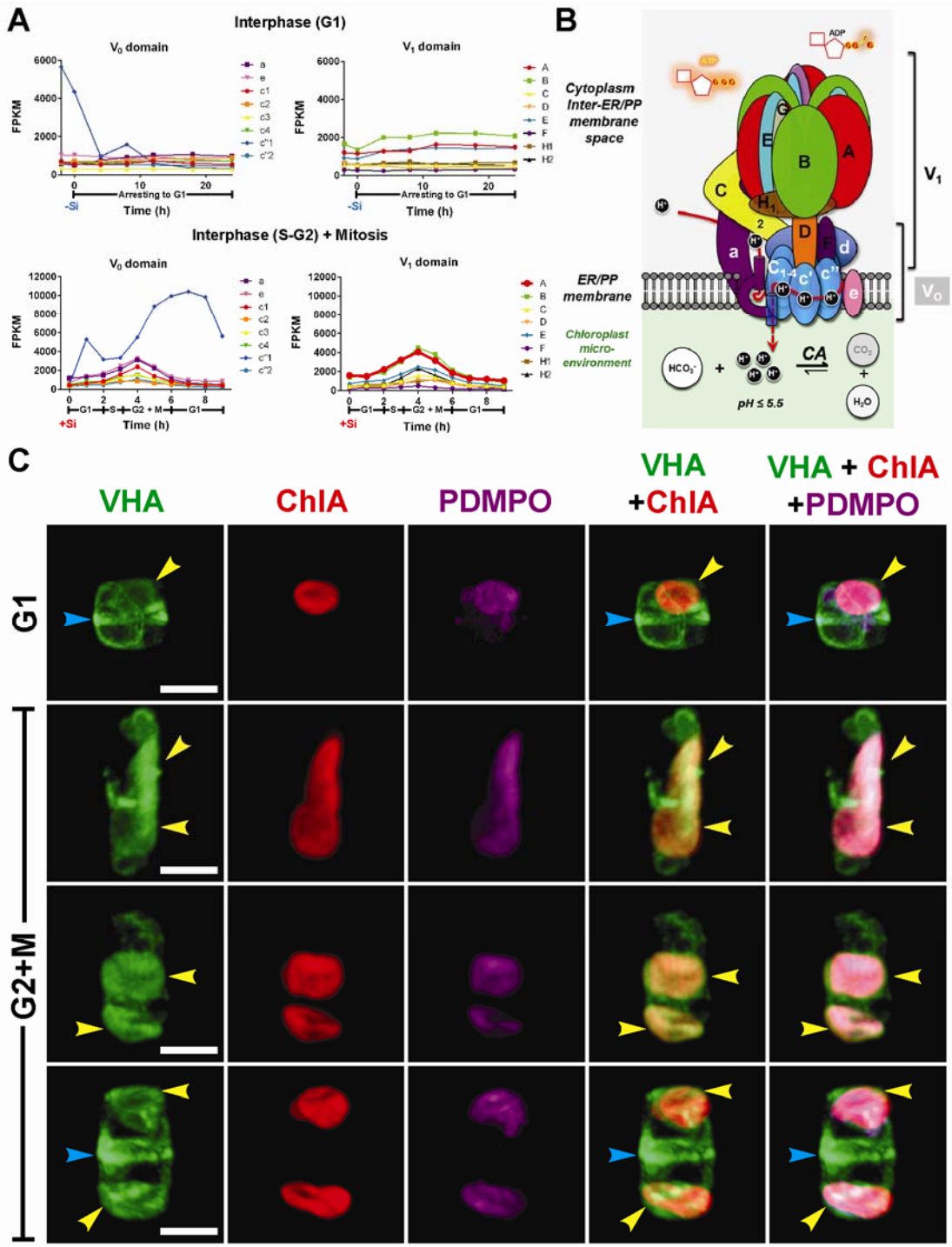

Fig. 2. Expression and subcellular localization of VHA in *T. pseudonana*. (**A**) Transcriptomic profile of VHA subunits during G1 (cell-cycle arrest following silicon starvation; top), and G2-S-G2 mitosis (synchronous division following silicon readdition; bottom). (**B**) Diagram of the VHA-holoenzyme complex in the endoplasmic reticulum/periplastid (ER/PP) membranes surrounding the chloroplast. CA = carbonic anhydrase. (**C**) 3D confocal images of eGFP-tagged VHA_B around chloroplasts (yellow arrows) co-localized with the acidotrophic dye PDMPO (magenta), and silica deposition vesicles (blue arrows) at different cell-cycle stages [scale bars: 5 μm].

We used NanoSIMS to quantify the effect of VHA inhibition on photosynthetic carbon fixation and incorporation into individual *T. pseudonana* cells following an 8h incubation with $NaH^{13}CO_3$. The isotope images revealed a statistically significant ~50% decrease in net biomass formation from photosynthesis in VHA-inhibited diatoms compared to controls (Fig. 3A-B).

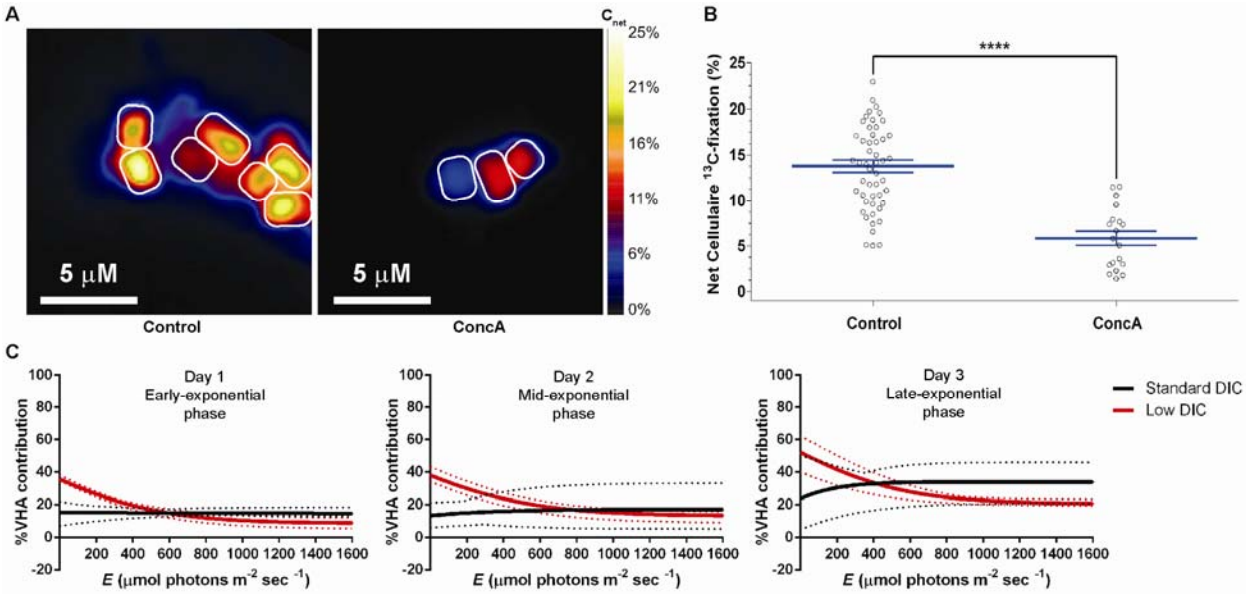

Fig. 3. Contribution of VHA to carbon fixation in *T. pseudonana*. (**A**, **B**) Single-cell NanoSIMS quantification of net biomass formation from photosynthesis in controls (n=51) and VHA-inhibited (concA= 10 nM concanamycin A) cells (n=19). Error bars = SEM; Paired *t* test: ****$p<0.0001$. (**C**) Contribution of VHA to bulk ^{14}C incorporation over the full range of oceanic irradiances, at three stages of growth, and at standard (1.92 mM; black lines; n=6) and low (1.60 mM; red lines; n=3) seawater DIC levels (dotted lines= 95% CI).

We conducted a more complete assessment of VHA-dependent photosynthetic carbon fixation by quantifying ^{14}C incorporation into *T. pseudonana* following 1h incubations with $NaH^{14}CO_3$. To capture the varying physiological status of cells during a diatom bloom (*23*), measurements were taken during early-, mid-, and late-exponential growth phases over three days of culturing (fig. S3). To assess the broad range of oceanic irradiances resulting from latitude, clouding, depth, and ocean mixing (*24*), photosynthesis vs. irradiance (P-E) incubations were curve fitted from 0-1600 μmols photons m^{-2} sec^{-1}. And to examine the response to rapid environmental DIC changes, incubations were conducted at ~2.0 mM (standard) and ~1.6 mM (low) DIC encompassing levels in the open ocean and coastal environments due to rainfall, ice melting, and terrestrial freshwater inputs (*25–27*) (fig. S4).

In our experiments, VHA inhibition impaired carbon fixation by at least 13.5% and as much as 52%. At standard DIC, the contribution of VHA to carbon fixation was relatively constant across irradiances ranging from ~15% on day 1 to ~29% on day 3 (Fig. 3C; black curves). At low DIC, VHA contribution also increased from day 1 to 3; however, it gained additional importance at irradiances under 500 μmols photons m^{-2} sec^{-1}. At sub-saturating irradiances <100 μmols photons m^{-2} sec^{-1}, the contribution of VHA to carbon fixation approached 40% on days 1-2 and surpassed 50% on day 3 of culturing (Fig. 3C; red curves). This pattern implies that VHA-enhancement of photosynthesis is most significant during DIC limitation and under light levels that match ocean depths where phytoplankton are most abundant (*28*).

In combination, the O_2 production, ^{13}C-NanoSIMS, and ^{14}C-P-E measurements demonstrate that VHA activity significantly contributes to photosynthetic fixing of carbon that is retained as biomass. Given that diatoms contribute nearly 50% of carbon fixation in the ocean (*29*, *30*), VHA-enhanced photosynthesis can be estimated to contribute between ~7 and 25% of oceanic primary production, or between 3.5 and 13.5 Gtons of fixed carbon per year (table S3). These numbers can only increase after accounting for analogous VHA-dependent mechanisms in other secondary endosymbiotic phytoplankton (Fig. 2) and tertiary photosymbiotic invertebrates (*12–14*).

Engulfment of food particles by phagocytosis followed by lysosomal digestion is ubiquitously used by eukaryotic cells (*9*), protozoans (*2*), and invertebrate animals (*31*). Acidification by VHA -which is conserved in all eukaryotes- is essential to these processes (*20*). The presence of VHA in membranes of phagocytic origin surrounding diatom chloroplasts and cnidarian endosymbiotic microalgae and its role in enhancing photosynthesis provide a functional link between phagocytosis, endosymbiosis and symbiogenesis. The symbiotic microalgae of giant clams are hosted in the gut lumen and therefore are extracellular; however, they are also surrounded by a host-derived VHA-containing membrane whose primary purpose is food digestion. Thus, VHA activity at the symbiosis interface constitutes a broader mechanism to enhance photosynthesis in phago-photosymbioses (Fig. 4). Acidification of the microenvironment surrounding the chloroplast or microalgae is bound to promote CO_2 accumulation, prevent CO_2 back-flow into the cytoplasm, and ultimately help saturate RuBisCO with CO_2 thus maximizing carbon fixation rates (*10*, *32*). Interestingly, the carbon concentrating mechanisms of diatoms, corals, and giant clams (*33–35*) all rely on carbonic anhydrases, and these enzymes form ubiquitously functional complexes with VHA to acidify intra- and extra-cellular compartments for diverse functions (*19*) including lysosomal (*36*) and epithelial digestion (*37*).

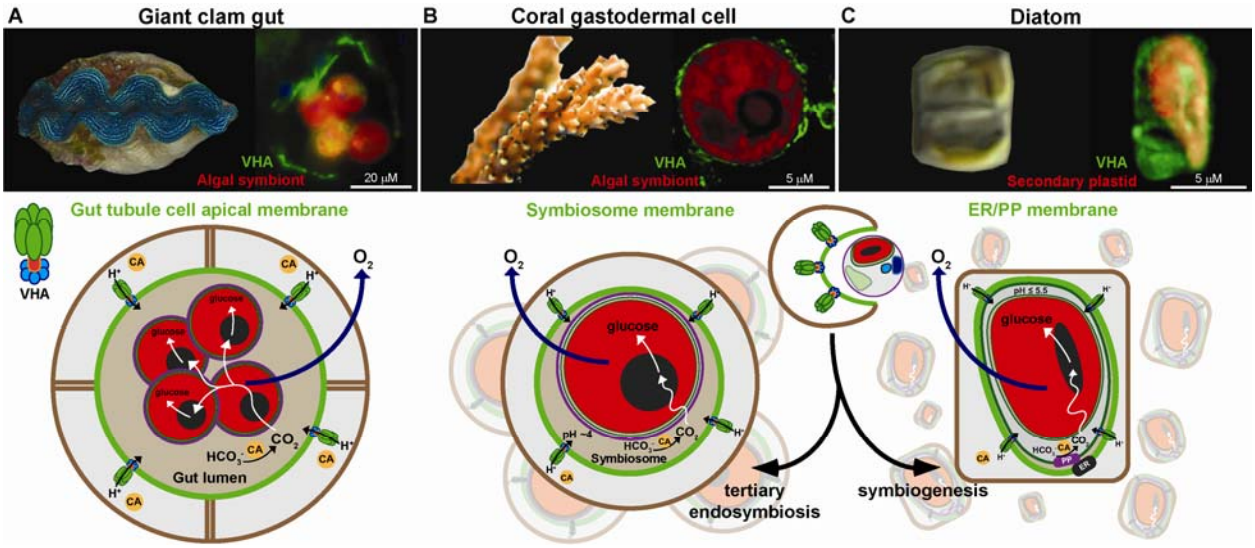

Fig. 4. Enhancement of photosynthesis by VHA in diverse marine phago-photosymbioses. VHA in the biological membrane at the photosymbiosis interface promotes photosynthesis at diverse stages of phago-photosymbiotic integration. (A) the apical membrane of epithelial cells in giant clam gut tubules that host microalgae extracellularly (*13*), (B) the symbiosomal membrane of coral gastrodermal cells that host microalgae intracellularly (*12*), and (C) the

endoplasmic reticulum/periplastid (ER/PP) membranes of diatoms that surround the plastid acquired from red microalgae by phagocytosis.

VHA-enhancement of photosynthesis co-opted from intracellular digestion confers a clear ecological advantage to extant marine secondary endosymbiotic phytoplankton. Since this advantage is also evident in extant tertiary photosymbiotic invertebrates, we speculate it was similarly important for the ancestral heterotrophic protist(s) that engulfed red microalgae during the transitional stages towards symbiogenesis. VHA-enhancement of photosynthesis would have provided a trait for positive selection and evolutionary advantage over other phytoplankton, particularly in the low-CO_2 Permian oceans where diatoms originated (*10*, *11*).

References and Notes

Acknowledgments: *We are grateful for the help of Dr. Roshan Shreshta, Dr. Brian Palenik, Dr. Orna Cook, Dr. Christopher Hewes, Dr. Garfield Kwan, Dr. Eric Armstrong and Mr. Angus Thies (details in Suppl. Text). Work at LLNL was performed under the auspices of US Department of Energy Office of Science contract DE-AC52-07NA27344. The confocal microscope at the Tresguerres laboratory was generously donated by the Arthur M. and Kate E. Tode Research Endowment in Marine Biological Sciences (UCSD).*

Funding:

National Institutes of Health grant T32GM067550 (DPY)

Ralph Lewin Graduate Fellowship (DPY)

LLNL Laboratory Directed Research and Development (LDRD) project # 19-LW-044 (TJS, XM)

SIO discretionary funds (MT)

Author contributions:

Conceptualization: DPY, MH, MT

Methodology: DPY, TJS, RMA, MV, XM, PKW, BGM, MH, MT

Investigation: DPY, TJS, BS, MH, MT

Visualization: DPY, TJS, MT

Funding acquisition: DPY, TJS, XM, PKW, MT

Project administration: DPY, MT

Resources: MH, MV, XM, BGM, MT

Supervision: MT

Writing – original draft: DPY, MT

Writing – review & editing: DPY, TJS, RMA, MV, PKW, XM, MT

Competing interests: *Authors declare that they have no competing interests.*

Data and materials availability: *The data discussed in this publication have been deposited in the NCBI's Gene Expression Omnibus and are accessible through GEO Series accession*

number GSE75460 (https://www.ncbi.nlm.nih.gov/geo/query/acc.cgi?acc=GSE75460) and GSE203136 (https://www.ncbi.nlm.nih.gov/geo/query/acc.cgi?acc=GSE203136).

Supplementary Materials

Materials and Methods

Supplementary Text

Figs. S1 to S5

Tables S1 to S3

References (39–47)